JMEPEG (2010) 19:591–598
DOI: 10.1007/s11665-009-9506-7

1059-9495/$19.00

Characterization of Atmospheric Corrosion of 2A12 Aluminum Alloy in Tropical Marine Environment

T. Li, X.G. Li, C.F. Dong, and Y.F. Cheng

(Submitted April 14, 2009; in revised form May 10, 2009)

In this work, corrosion product formed on 2A12 aluminum (Al) alloy after 3 months of natural exposure in South China Sea atmosphere was characterized by various surface analysis techniques, including scanning electron microscopy, energy-dispersive x-ray analysis, x-ray photoelectron spectroscopy, and x-ray diffraction. The atmospheric corrosion mechanism of Al alloy in marine environment was derived. Results demonstrated that Al alloy specimen experiences serious general corrosion and pitting corrosion. Al and O are enriched in the product film, and Ca and Cl are also found in the film and corrosion pits in Al alloy substrate. The main component compounds existing in the film include Al_2O_3, $Al(OH)_3$, and AlOOH while $AlCl_3$ and $CaCO_3$ are also identified. Al alloy encounters corrosion under tropical marine atmosphere. Although somewhat protective, the formed surface film on Al alloy specimen is attacked by chloride ions, resulting in significant pitting corrosion of Al alloy.

Keywords aluminum alloy, corrosion, marine atmosphere, surface analysis

1. Introduction

Atmospheric corrosion is one of the most common types of corrosion to degrade metallic structures, devices, and products exposed to atmosphere. Atmospheric conditions such as relative humidity, temperature, sunshine period, pollutants, salinity, etc. play an essential role in corrosion of the exposed metals (Ref 1). In particular, tropical and subtropical marine environment introduces one of the most aggressive conditions to result in serious atmospheric corrosion of metals.

The Xi-Sha islands, located in the northwest of South China Sea, is characterized with extreme environmental conditions, such as high temperature, high humidity, high salinity, and long-time sunshine. Investigation of atmospheric corrosion behavior of metals is essential to ensure integrity and safety of structural materials used under such a typical climate. To date, there has been no relevant work directly conducted in the atmospheric station.

Aluminum (Al) and its alloys have been used extensively in various industrial applications due to their light weight, high strength, and good corrosion resistance (Ref 2, 3). In particular, 2A12 Al alloy has been widely used as structural material in aeronautical industries (Ref 4). Generally, corrosion resistance of Al alloy is mainly attributed to formation of a layer of oxide film or corrosion product scale on its surface (Ref 5, 6). The composition, structure, and morphology of the corrosion product layer play an important role in the subsequent corrosion of Al alloy under film/scale. Natesan et al. (Ref 1) studied atmospheric corrosion behavior of metals including galvanized iron and Al in Indian marine, industrial, urban, and rural environments by weight-loss method over a period of 5 years. They found that the corrosion loss of metals is strongly dependent on the location where the specimens are exposed. Moreover, a linear relationship was observed between weight-loss of Al and the exposure time. Mendoza and Corvo (Ref 7) characterized atmospheric corrosion of copper, zinc, and Al exposed indoor and outdoors (coastal, urban-industrial, and rural) up to 18 months, and established empirical equations to predict atmospheric corrosion rates of metals. Corvo et al. (Ref 8) performed corrosion research on copper, zinc, and Al exposed at three humid-tropical atmospheric environments in Cuba and Campeche. Their results show that metals exposed to sheltered conditions presented higher corrosion rates compared to outdoors, whereas in closed (indoor) environments the corrosion rate significantly decreased. Morcillo et al. (Ref 9) summarized corrosion rates of steel, zinc, copper, and Al exposed at three Antarctic sites and detailed the morphology of corrosion products formed in the Antarctic region. Vera et al. (Ref 10) evaluated the combined effect of marine and industrial pollutants on atmospheric corrosion of Al and 6201 Al alloy. Good correlation was obtained between weight-loss, corrosion depth and time, and pollutant contents. Fuente et al. (Ref 11) also reported corrosion data and morphology of corrosion products formed on Al panels after 13 to 16 years of exposure under various types of atmosphere in Spain.

The 2A12 Al alloy has been used extensively in tropical marine environment in South China. Despite the extensive studies of corrosion and atmospheric corrosion of Al alloy as summarized above, none of them was conducted under condition specific to the environment typical of South China

T. Li, Corrosion and Protection Center, University of Science and Technology Beijing, Beijing 100083, China and School of Materials & Metallurgy, Inner Mongolia University of Science and Technology, Baotou 014010, China; **X.G. Li** and **C.F. Dong**, Corrosion and Protection Center, University of Science and Technology Beijing, Beijing 100083, China; and **Y.F. Cheng**, Department of Mechanical & Manufacturing Engineering, University of Calgary, Calgary, AB T2N 1N4, Canada. Contact e-mails: lixiaogang99@263.net and fcheng@ucalgary.ca.

Sea. Therefore, the corrosion mechanism of 2A12 Al alloy under the typical environmental condition has remained unclear.

In this work, corrosion product formed on 2A12 Al alloy after 3 months of exposure in South China Sea atmosphere was characterized by various surface analysis techniques, including scanning electron microscopy (SEM), energy-dispersive x-ray analysis (EDXA), x-ray photoelectron spectroscopy (XPS), and x-ray diffraction (XRD). The mechanism for atmospheric corrosion of Al alloy in the tropical marine environment was analyzed. The authors realized that the atmospheric exposure usually took 1 year or more for a study cycle. The reported work was thus a part of research program in this area. Furthermore, it is worthy pointing out that there is no typical four-season climate in the test location. The reported results in this work reflect an exposure of 3 months, which are representative of the climate environment in a year.

2. Experimental

Specimens for atmospheric corrosion tests were cut from a sheet of 2A12 Al alloy, with the chemical composition (wt.%): 0.13 Si, 0.35 Fe, 4.68 Cu, 0.53 Mn, 1.58 Mg, 0.10 Zn, and 0.023 Ti. The specimens with a dimension of 100 mm × 50 mm × 3 mm were ground with SiC papers sequentially to 800 grit and then degreased by acetone followed by cleaning in ethanol. After drying and weighting, the specimens were installed on the atmospheric corrosion exposure supporter at an angle of 45° relative to the ground (Ref 12). The exposure supporter was located in a big square, avoiding shadows of trees and blocking by building. The distance between the exposure field and the seashore line was 150 m, and the atmospheric exposure time period was 3 months.

The climatic parameters of Xi-Sha islands including temperature, relative humidity, rainfall, SO_2 pollutant amount, and air-borne salinity represented by chloride were provided by meteorological observatory stations monthly.

After 3 months of exposure, the specimens were collected and dried in desiccators. The surface morphology and elemental composition of corrosion product formed were analyzed using a JSM6480LV SEM, coupled to a Noran System Six EDXA. Furthermore, the corrosion product was characterized with a MART 2 XPS and XRD.

3. Results

3.1 Climate of Xi-Sha Islands

Xi-Sha islands, where the atmospheric corrosion exposure station was built, is located in the northwest of South China Sea (111°-113°E, 15°30′-17°0′ N) (Ref 13). There is an annual average air temperature of 27 °C, and an average relative humidity of about 82%, with the maximum relative humidity approaching 100% and the minimum value of 47%. The air-borne salinity content, depending on wind rate and distance from the shore line, is about 0.3 to 1.5 mg/m^3 in average. With an average annual wind rate of about 4.3 m/s with a maximum of 36 m/s, seawater collides and flies over reef and shoreline, leading to a very high chloride deposition rate, with an average diameter of NaCl particles of about 10 μm.

3.2 Surface Morphologies of Corrosion Product and Al Alloy Substrate

Figure 1 shows the optical views of macroscopic morphology of the top and bottom parts of Al alloy specimen after 3 months of atmospheric exposure. It is clear that the specimen was heavily corroded, with localized corrosion occurring on specimen surface. Both views show that the specimen lost brightness and became rough, with a yellowish gray patina present on the surface. Moreover, corrosion of Al alloy specimen on bottom was much more serious than that on top part.

Figure 2 shows the SEM images of microscopic morphology of the specimen. It is seen that tiny particles with hemispherical shape were scattered on the surface of specimen. The corrosion product formed on bottom specimen was composed of dark-gray compact layer and relatively loose white surface layer, while that on the top was loose, cracked white layer.

The morphology of Al alloy substrate on removal of corrosion product layer is shown in Fig. 3. Apparently, the bottom part was more corroded than the top. Moreover, isolated pits were observed on the specimen surface. Pits formed on the top were generally smaller and shallower than those present in bottom part of specimen.

Figure 4 shows the SEM images of polished transverse cross-section of specimen. It is seen that corrosion product layer formed on bottom specimen (Fig. 4a) was compact and continuous. It generally consisted of two layers (Fig. 4c), with the thickness of outer loose layer of about 10 μm, and the inner compact layer of 30 μm. Corrosion product layer formed on top specimen was noncontinuous (Fig. 4b), with a maximum thickness of about 10 μm.

Furthermore, the cross-section views of specimen also revealed the existence of isolated corrosion pits in Al alloy substrate (Fig. 4c). The shallow, hemispherical pits were also observed in both bottom and top parts of specimen (Fig. 4d, e).

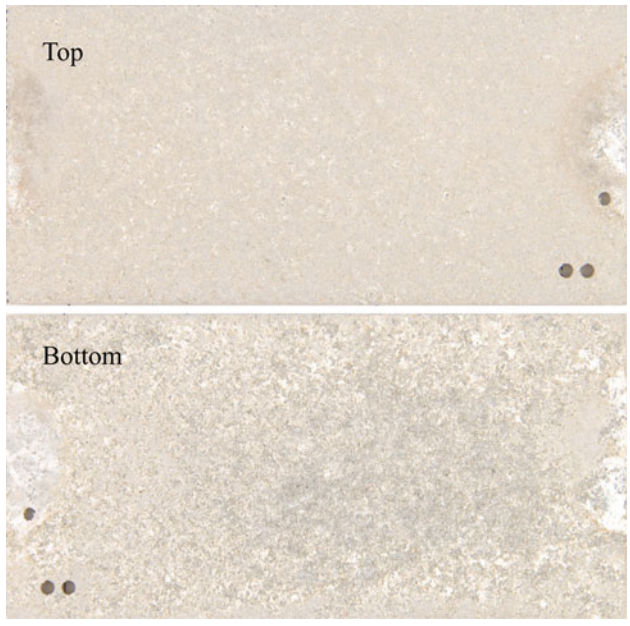

Fig. 1 Optical views of surface morphology of top and bottom parts of Al alloy specimen after 3 months of exposure in Xi-Sha Island atmosphere

With development of corrosion pits, intergranular attack occurred, as seen in Fig. 4(d) and (e).

3.3 Determination of Elemental Distribution in Corrosion Product

Figure 5 shows the EDXA of corrosion product and the white surface layer on specimen surface after 3 months of exposure. It is seen that the dominant elements in corrosion product were Al and O.

Figure 6 shows the EDXA measured at points 1, 2, and 3 in Fig. 4(c), where point 1 refers the outer layer and points 2 and 3 refer to the inner surface film. It is seen that element Ca was enriched in the outer layer, while the dominant elements in inner film were O and Al.

Figure 7 shows the EDXA results measured at corrosion pits formed on Al alloy substrate under surface film indicated in Fig. 4(e). In addition to a significant amount of Cl, O was also detected, but with a much lower amount than that existing in the film (Fig. 5). Moreover, Cl was found to be present in corrosion pits.

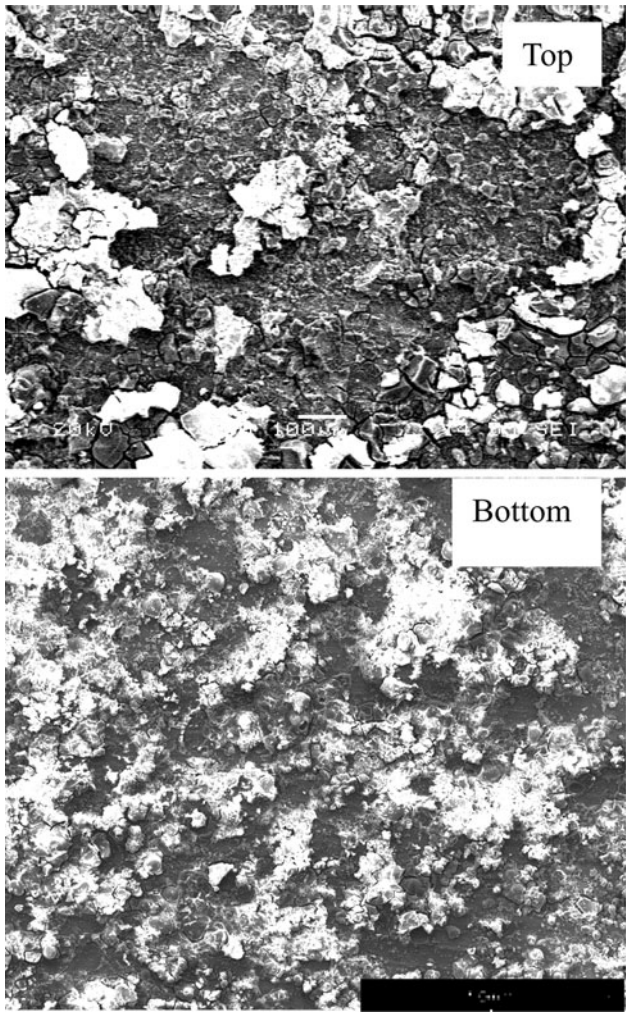

Fig. 2 SEM views of surface morphology of top and bottom parts of Al alloy specimen after 3 months of exposure in Xi-Sha Island atmosphere

3.4 Structural Characterization of Corrosion Product

Figure 8 exhibits XPS results of corrosion product formed on Al alloy surface after 3 months of atmospheric exposure. It is seen that spectra of Al2P and O1s showed distinct peaks at about 74 and 531 eV, respectively. The peak of Na1s was observed at 1071.2 eV, which was mainly from NaCl since the reference spectrum energy was 1072.1 eV. Moreover, the weak peaks of $Cl2p_{1/2}$, $Cl2p_{3/2}$, $Ca2p_{1/2}$, and $Ca2p_{3/2}$ were found at 198.66, 202.61, 351.33, and 347.22 eV, respectively. From XPS and EDXA results, it is expected that the corrosion product on Al alloy specimen possibly consisted of $[Al(OH)_3]$ (bayerite), Al_2O_3, AlOOH, and chloride-containing product such as $AlCl_3$, $CaCO_3$, etc.

Figure 9 shows the XRD pattern of corrosion product formed on Al alloy specimen after 3 months of exposure. According to the standard diffraction angle, the products Al, $AlCl_3$, Al_2O_3, $Al(OH)_3$, AlOOH, and $CaCO_3$ were identified. The result was consistent with the XPS/EDXA very well.

4. Discussion

4.1 Atmospheric Corrosion of Al Alloy and Formation of Aluminum Oxide Film

Atmospheric corrosion of metal, including Al and Al alloy, is strongly dependent on presence of moisture or thin aqueous solution film on metal surface. When pollutant gases and/or salt ions are dissolved, a layer of electrolyte is generated, and corrosion of metal is resulted in. Under high temperature, high-humidity tropical condition, corrosion of Al alloy is expected,

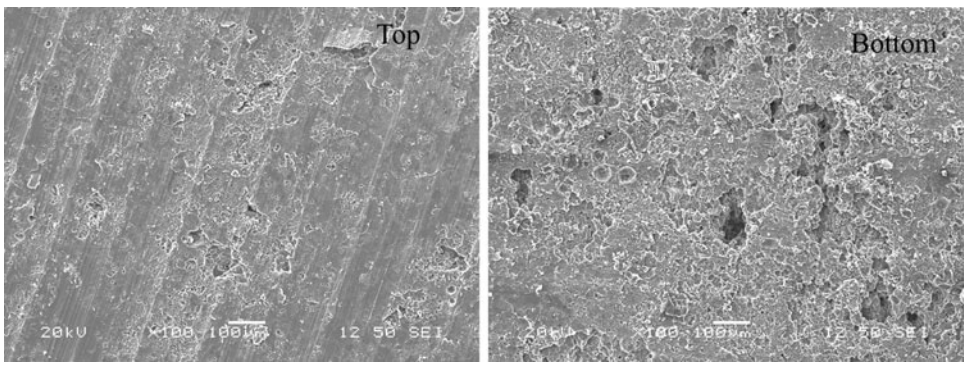

Fig. 3 SEM views of Al alloy substrate after corrosion product removal

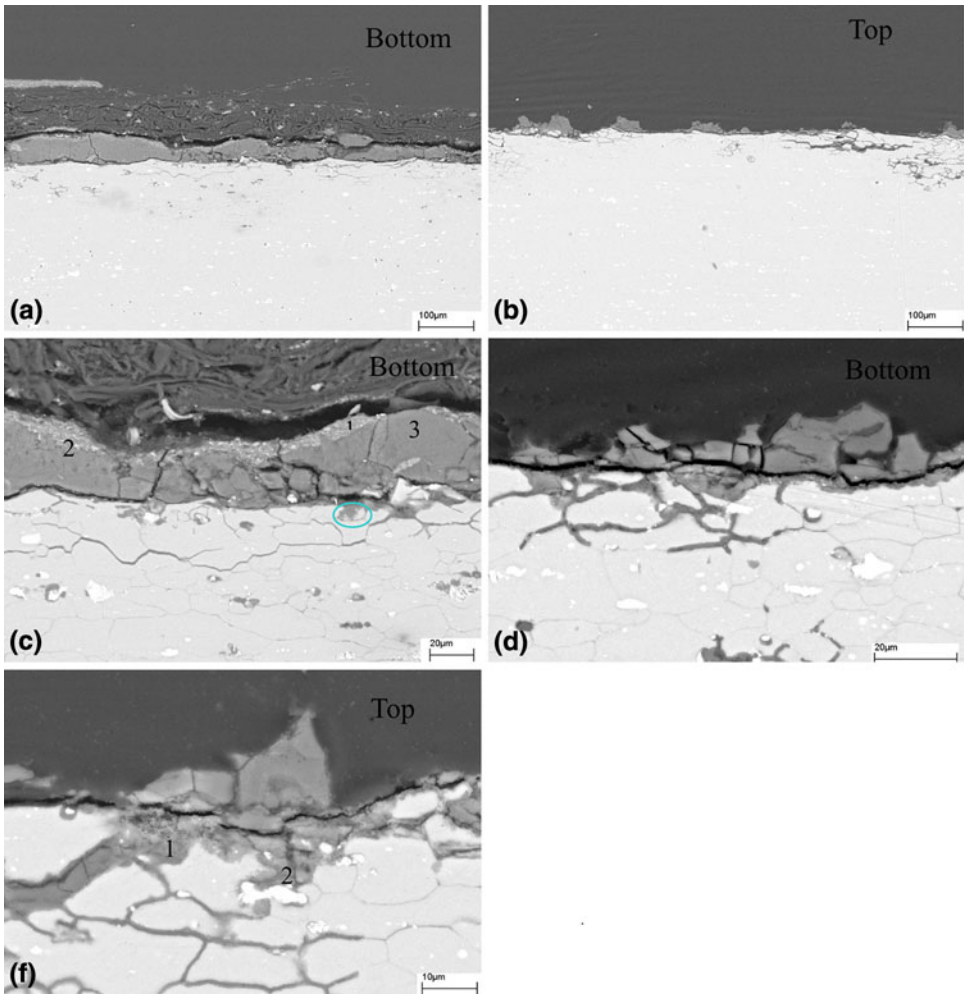

Fig. 4 SEM views of morphology of top and bottom parts of Al alloy specimen with various magnifications after 3 months of exposure in Xi-Sha islands atmosphere, where $c_{1,2,3}$ refer to different locations in film formed on the bottom specimen, and $e_{1,2}$ indicate the corrosion pits formed on top part of Al alloy substrate

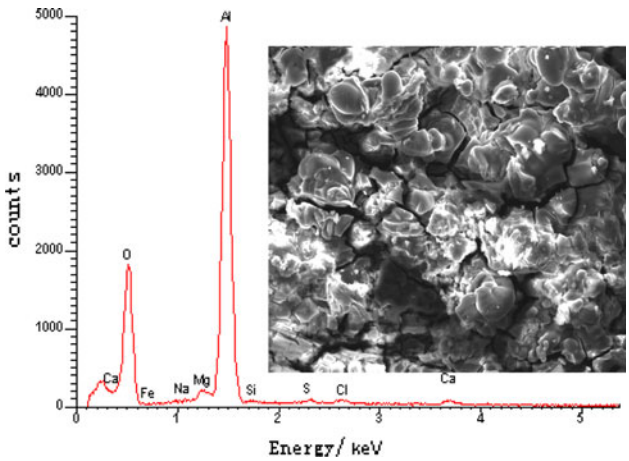

Fig. 5 EDXA result measured on Al alloy specimen after 3 months of exposure in Xi-Sha Island atmosphere

with oxidation of Al alloy as anodic reaction and reduction of dissolved oxygen as cathodic reaction:

$$Al \rightarrow Al^{3+} + 3e \quad \text{(Eq 1)}$$

$$O_2 + 2H_2O + 4e \rightarrow 4OH^- \quad \text{(Eq 2)}$$

Thus, Al alloy will be oxidized into $Al(OH)_3$ by

$$4Al + 3O_2 + 6H_2O \rightarrow 4Al(OH)_3 \quad \text{(Eq 3)}$$

Moreover, due to the presence of a thin electrolyte layer, it is quite easy to achieve the saturation solubility of $Al(OH)_3$. At near-neutral pH electrolyte, the following chemical reaction occurs:

$$Al^{3+} + 3OH^- \rightarrow Al(OH)_3 \quad \text{(Eq 4)}$$

$Al(OH)_3$ would be further transformed into

$$2Al(OH)_3 \rightarrow Al_2O_3 + 3H_2O \quad \text{(Eq 5)}$$

Therefore, oxide films formed on Al alloy in near-neutral pH atmospheric environment generally consists of boehmite (AlOOH), bayerite ($Al(OH)_3$), and Al_2O_3, as identified in this work.

With a position of 45° relative to the ground, it is expected that there is a higher moisture or water content on bottom part of specimen than that on the top. The moisture or water could be from either rain remnant or dew. The temperature cycle from sunshine in the daytime would result in evaporation of moisture

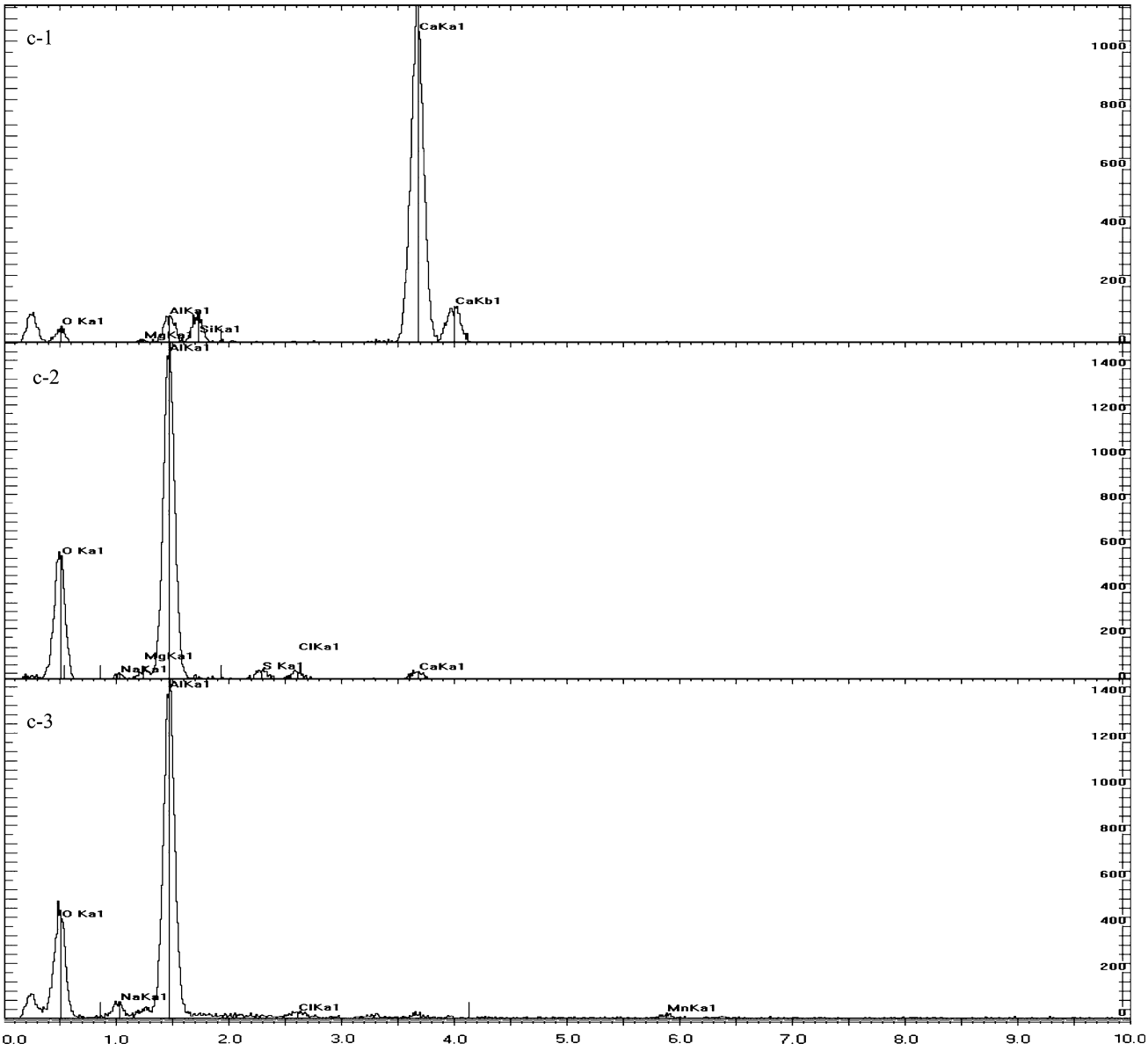

Fig. 6 EDXA results measured at points 1, 2, and 3 in Fig. 4(c)

from the specimen. Therefore, the top specimen will remain dry for a longer time period than the bottom. As a consequence, corrosion will be more serious at the bottom part of Al alloy specimen. Furthermore, with more corrosion of Al alloy at the bottom, more Al^{3+} generates. Consequently, a thicker, more compact corrosion product film is resulted in compared to that formed at the top part.

A double-layer film structure is found to form on Al alloy surface during atmospheric exposure, with the inner layer of compact Al oxide film and the outer layer of noncontinuous contaminated layer. The similar structure was found by Ferrer and Kelly (Ref 14). The deposit of dust is preferentially formed on the outermost layer. Ca and Si identified by EDXA are mainly from the atmospheric dust.

4.2 Pitting Corrosion of Al Alloy in Marine Atmosphere

It has been generally acknowledged (Ref 15-17) that the presence of chloride ions in environment results in pitting corrosion of Al alloy. Due to the high content of chloride ions existing in Xi-Sha islands atmosphere, pitting of Al alloy specimen is thus highly expected. Chlorine enters the surface film via the deposition of sea salt and rain precipitation. There have been several mechanisms illustrating the role of chloride ions in pitting corrosion of passivated metals like Al alloy (Ref 5, 6, 18, 19). According to point defect model (Ref 17), chloride ions would compete with cation vacancies and replace oxygen in the oxide film to form metal chlorine, resulting in degradation of oxide film and initiation of pitting.

Aluminum chloride identified in this work provides proof that chloride ions will react with cation, such as Al^{3+}, to form chloride-containing compound. Mechanisms are proposed to describe the formation of aluminum chloride (Ref 20):

$$Al(OH)_3 + 3Cl^- \rightarrow AlCl_3 + 3OH^- \quad \text{(Eq 6)}$$

The presence of a significant amount of Cl in corrosion pits (Fig. 7) and identification of $AlCl_3$ in surface film (Fig. 9)

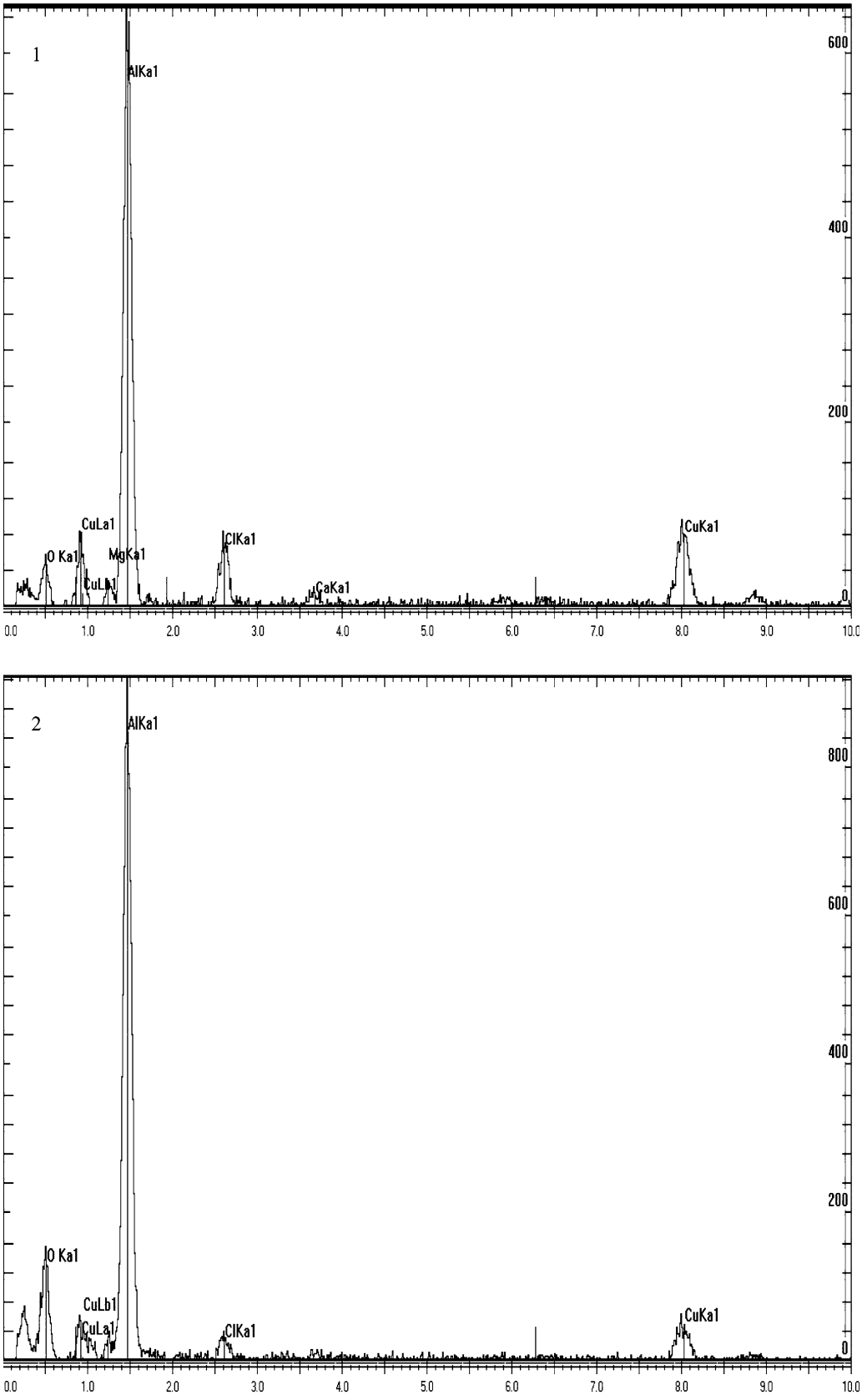

Fig. 7 EDXA results measured at points 1 and 2 in Fig. 4(e)

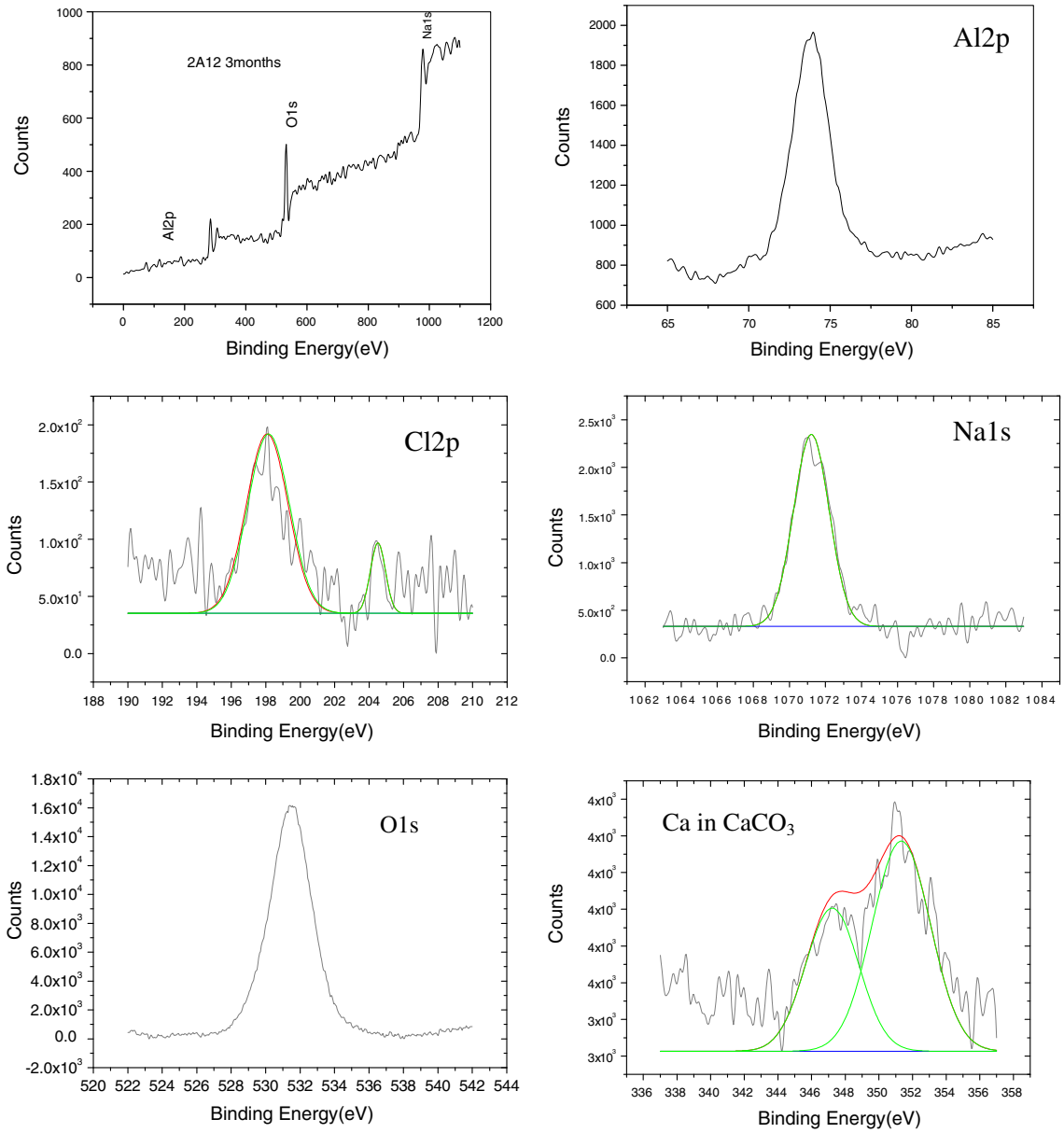

Fig. 8 XPS spectra measured on corrosion product formed on Al alloy specimen after 3 months of exposure in Xi-Sha Islands atmosphere

formed under X-Sha Island atmosphere show that chloride ions are incorporated into oxide film and results in pit initiation.

Furthermore, pitting occurring in bottom part of Al alloy specimen is much more serious than that in top specimen (Fig. 3). Apparently, occurrence of pitting corrosion is also dependent on the presence of an aqueous electrolyte layer on electrode surface. The longer the solution layer remains, the more serious both general corrosion and pitting corrosion will be.

5. Conclusions

Al alloy specimen exposed under marine atmosphere experiences serious general corrosion and pitting corrosion. In particular, the bottom part of the specimen is more corroded than the top part, and there are bigger and deeper pits formed in bottom specimen than in the top.

Corrosion product film was more compact and continuous on bottom than that on the top. Al and O are enriched in the product film, and Ca and Al are also found in the film and corrosion pits in the Al alloy substrate. The main component compounds existing in surface film include Al_2O_3, $Al(OH)_3$, and AlOOH while $AlCl_3$ and $CaCO_3$ are also identified.

Al alloy encounters corrosion under tropical marine atmosphere. Although somewhat protective, the formed surface film on Al alloy specimen is attacked by chloride ions, resulting in significant pitting corrosion of Al alloy.

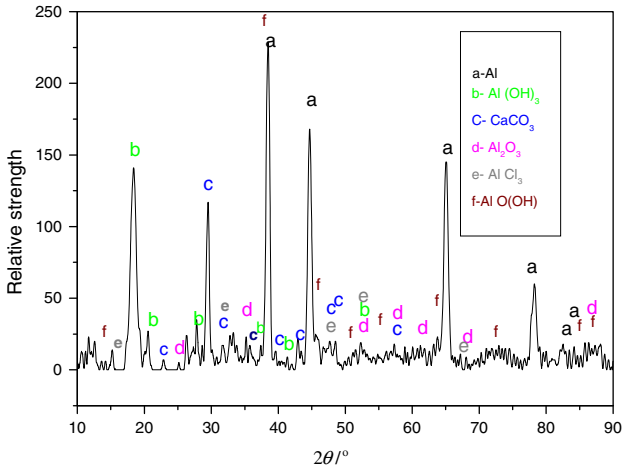

Fig. 9 XRD of corrosion product formed on Al alloy specimen after 3 months of exposure in Xi-Sha Islands atmosphere

Acknowledgments

This work was supported by the Ministry of Science and Technology of China (Project No. 2005DKA10400) and Canada Research Chairs Program.

References

1. M. Natesan, G. Venkatachari, and N. Palaniswamy, Kinetics of Atmospheric Corrosion of Mild Steel, Zinc, Galvanized Iron and Aluminum at 10 Exposure Stations in India, *Corros. Sci.*, 2006, **48**, p 3584
2. L. Chen, N. Myung, P.T.A. Sumodjo, and K. Nobe, A Comparative Electrodissolution and Localized Corrosion Study of 2024A1 in Halide Media, *Electrochim. Acta*, 1999, **44**, p 2751
3. V. Guillaumin and G. Mankowski, Corrosion of 2024 T351 Aluminum Alloy in Chloride Media, *Corros. Sci.*, 1999, **41**, p 421
4. K.-H. Na and S.-I. Pyun, Effects of Sulphate, Nitrate and Phosphate on Pit Initiation of Pure Aluminum in HCl-Based Solution, *Corros. Sci.*, 2007, **48**, p 2663
5. Z. Szklarska-Smialowska, Pitting Corrosion of Aluminum, *Corros. Sci.*, 1999, **41**, p 1743
6. G.S. Frankel, Pitting Corrosion of Metals; A Summary of the Critical Factors, *J. Electrochem. Soc.*, 1998, **145**, p 2186
7. A.R. Mendoza and F. Corvo, Outdoor and Indoor Atmospheric Corrosion of Non-Ferrous Metals, *Corros. Sci.*, 2000, **42**, p 1123
8. F. Corvo, T. Perez, L.R. Dzib, Y. Martinc, A. Castaneda, E. Gonzalez, and J. Perez, Outdoor–Indoor Corrosion of Metals in Tropical Coastal Atmospheres, *Corros. Sci.*, 2008, **50**, p 220
9. M. Morcillo, B. Chico, D. De La Fuente, E. Almeida, G. Joseph, S. Rivero, and B. Rosales, Atmospheric Corrosion of Reference Metals in Antarctic Sites, *Cold Regions Sci. Technol.*, 2004, **40**, p 165
10. R. Vera, D. Delgado, and B.M. Rosales, Effect of Atmospheric Pollutants on the Corrosion of High Power Electrical Conductors: Part 1. Aluminum and AA6201 Alloy, *Corros. Sci.*, 2006, **48**, p 2882
11. D. de la Fuente, E. Otero-Huerta, and M. Morcillo, Studies of Long-Term Weathering of Aluminium in the Atmosphere, *Corros. Sci.*, 2007, **49**, p 3134
12. "Standard Practice for Conducting Atmospheric Corrosion Tests on Metals," ASTM G50-76, ASTM, 2003
13. J. Liu, Z. Ye, C. Han, X. Liu, and G. Qu, Meteoric Diagenesis in Pleistocene Reef Limestones of Xi-Sha Islands, China, *J. Asian Earth Sci.*, 1997, **15**, p 465
14. K.S. Ferrer and R.G. Kelly, Comparison of Methods of Removal of Corrosion Products from AA20424-T3, *Corrosion*, 2001, **57**, p 110
15. T.T. Lunt, J.R. Scully, V. Brusamarello, A.S. Mikhailov, and J.L. Hudson, Spatial Interactions Among Localized Corrosion Sites: Experiments and Modeling, *J. Electrochem. Soc.*, 2002, **149**, p B163
16. A.M. Lucente and J.R. Scully, Pitting and Alkaline Dissolution of an Amorphous–Nanocrystalline Alloy with Solute-Lean Nanocrystals, *Corros. Sci.*, 2007, **49**, p 2351
17. D.D. Macdonald, The Point Defect Model for the Passive State, *J. Electrochem. Soc.*, 1992, **139**, p 3434
18. T.-S. Huang, S. Zhao, G.S. Frankel, and D.A. Wolfe, A Statistical Model for Localized Corrosion in 7xxx Aluminum Alloys, *Corrosion*, 2007, **65**, p 819
19. C.J. Boxley, J.J. Watkins, and H.S. White, Corrosion Behavior on Aluminum Alloy LY12 in Simulated Atmospheric Corrosion Process, *Electrochem. Solid State Lett.*, 2003, **6**, p B38
20. A.S. Elola, T.F. Otero, and A. Porro, Evolution of the Pitting of Aluminum Exposed to the Atmosphere, *Corrosion*, 1992, **48**, p 854